DESY 06-038
April 2006

ISSN 0418-9833

Search for Doubly-Charged Higgs Boson Production at HERA

H1 Collaboration

Abstract

A search for the single production of doubly-charged Higgs bosons $H^{\pm\pm}$ in ep collisions is presented. The signal is searched for via the Higgs decays into a high mass pair of same charge leptons, one of them being an electron. The analysis uses up to 118 pb^{-1} of ep data collected by the H1 experiment at HERA. No evidence for doubly-charged Higgs production is observed and mass dependent upper limits are derived on the Yukawa couplings h_{el} of the Higgs boson to an electron-lepton pair. Assuming that the doubly-charged Higgs only decays into an electron and a muon via a coupling of electromagnetic strength $h_{e\mu} = \sqrt{4\pi\alpha_{em}} = 0.3$, a lower limit of 141 GeV on the $H^{\pm\pm}$ mass is obtained at the 95% confidence level. For a doubly-charged Higgs decaying only into an electron and a tau and a coupling $h_{e\tau} = 0.3$, masses below 112 GeV are ruled out.

Submitted to *Phys. Lett. B*

A. Aktas[9], V. Andreev[25], T. Anthonis[3], B. Antunovic[26], S. Aplin[9], A. Asmone[33], A. Astvatsatourov[3], A. Babaev[24,†], S. Backovic[30], A. Baghdasaryan[37], P. Baranov[25], E. Barrelet[29], W. Bartel[9], S. Baudrand[27], S. Baumgartner[39], J. Becker[40], M. Beckingham[9], O. Behnke[12], O. Behrendt[6], A. Belousov[25], N. Berger[39], J.C. Bizot[27], M.-O. Boenig[6], V. Boudry[28], J. Bracinik[26], G. Brandt[12], V. Brisson[27], D. Bruncko[15], F.W. Büsser[10], A. Bunyatyan[11,37], G. Buschhorn[26], L. Bystritskaya[24], A.J. Campbell[9], F. Cassol-Brunner[21], K. Cerny[32], V. Cerny[15,46], V. Chekelian[26], J.G. Contreras[22], J.A. Coughlan[4], B.E. Cox[20], G. Cozzika[8], J. Cvach[31], J.B. Dainton[17], W.D. Dau[14], K. Daum[36,42], Y. de Boer[24], B. Delcourt[27], M. Del Degan[39], A. De Roeck[9,44], E.A. De Wolf[3], C. Diaconu[21], V. Dodonov[11], A. Dubak[30,45], G. Eckerlin[9], V. Efremenko[24], S. Egli[35], R. Eichler[35], F. Eisele[12], A. Eliseev[25], E. Elsen[9], S. Essenov[24], A. Falkewicz[5], P.J.W. Faulkner[2], L. Favart[3], A. Fedotov[24], R. Felst[9], J. Feltesse[8], J. Ferencei[15], L. Finke[10], M. Fleischer[9], G. Flucke[33], A. Fomenko[25], G. Franke[9], T. Frisson[28], E. Gabathuler[17], E. Garutti[9], J. Gayler[9], C. Gerlich[12], S. Ghazaryan[37], S. Ginzburgskaya[24], A. Glazov[9], I. Glushkov[38], L. Goerlich[5], M. Goettlich[9], N. Gogitidze[25], S. Gorbounov[38], C. Grab[39], T. Greenshaw[17], M. Gregori[18], B.R. Grell[9], G. Grindhammer[26], C. Gwilliam[20], D. Haidt[9], L. Hajduk[5], M. Hansson[19], G. Heinzelmann[10], R.C.W. Henderson[16], H. Henschel[38], G. Herrera[23], M. Hildebrandt[35], K.H. Hiller[38], D. Hoffmann[21], R. Horisberger[35], A. Hovhannisyan[37], T. Hreus[3,43], S. Hussain[18], M. Ibbotson[20], M. Ismail[20], M. Jacquet[27], L. Janauschek[26], X. Janssen[3], V. Jemanov[10], L. Jönsson[19], D.P. Johnson[3], A.W. Jung[13], H. Jung[19,9], M. Kapichine[7], J. Katzy[9], I.R. Kenyon[2], C. Kiesling[26], M. Klein[38], C. Kleinwort[9], T. Klimkovich[9], T. Kluge[9], G. Knies[9], A. Knutsson[19], V. Korbel[9], P. Kostka[38], K. Krastev[9], J. Kretzschmar[38], A. Kropivnitskaya[24], K. Krüger[13], M.P.J. Landon[18], W. Lange[38], G. Laštovička-Medin[30], P. Laycock[17], A. Lebedev[25], G. Leibenguth[39], V. Lendermann[13], S. Levonian[9], L. Lindfeld[40], K. Lipka[38], A. Liptaj[26], B. List[39], J. List[10], E. Lobodzinska[38,5], N. Loktionova[25], R. Lopez-Fernandez[23], V. Lubimov[24], A.-I. Lucaci-Timoce[9], H. Lueders[10], D. Lüke[6,9], T. Lux[10], L. Lytkin[11], A. Makankine[7], N. Malden[20], E. Malinovski[25], S. Mangano[39], P. Marage[3], R. Marshall[20], L. Marti[9], M. Martisikova[9], H.-U. Martyn[1], S.J. Maxfield[17], A. Mehta[17], K. Meier[13], A.B. Meyer[9], H. Meyer[36], J. Meyer[9], V. Michels[9], S. Mikocki[5], I. Milcewicz-Mika[5], D. Milstead[17], D. Mladenov[34], A. Mohamed[17], F. Moreau[28], A. Morozov[7], J.V. Morris[4], M.U. Mozer[12], K. Müller[40], P. Murín[15,43], K. Nankov[34], B. Naroska[10], Th. Naumann[38], P.R. Newman[2], C. Niebuhr[9], A. Nikiforov[26], G. Nowak[5], K. Nowak[40], M. Nozicka[32], R. Oganezov[37], B. Olivier[26], J.E. Olsson[9], S. Osman[19], D. Ozerov[24], V. Palichik[7], I. Panagoulias[9], T. Papadopoulou[9], C. Pascaud[27], G.D. Patel[17], H. Peng[9], E. Perez[8], D. Perez-Astudillo[22], A. Perieanu[9], A. Petrukhin[24], D. Pitzl[9], R. Plačakytė[26], B. Portheault[27], B. Povh[11], P. Prideaux[17], A.J. Rahmat[17], N. Raicevic[30], P. Reimer[31], A. Rimmer[17], C. Risler[9], E. Rizvi[18], P. Robmann[40], B. Roland[3], R. Roosen[3], A. Rostovtsev[24], Z. Rurikova[26], S. Rusakov[25], F. Salvaire[10], D.P.C. Sankey[4], E. Sauvan[21], S. Schätzel[9], S. Schmidt[9], S. Schmitt[9], C. Schmitz[40], L. Schoeffel[8], A. Schöning[39], H.-C. Schultz-Coulon[13], F. Sefkow[9], R.N. Shaw-West[2], I. Sheviakov[25], L.N. Shtarkov[25], Y. Sirois[28], T. Sloan[16], P. Smirnov[25], Y. Soloviev[25], D. South[9], V. Spaskov[7], A. Specka[28], M. Steder[9], B. Stella[33], J. Stiewe[13], A. Stoilov[34], U. Straumann[40], D. Sunar[3], V. Tchoulakov[7], G. Thompson[18], P.D. Thompson[2], T. Toll[9], F. Tomasz[15], D. Traynor[18], P. Truöl[40], I. Tsakov[34], G. Tsipolitis[9,41], I. Tsurin[9], J. Turnau[5], E. Tzamariudaki[26], K. Urban[13], M. Urban[40], A. Usik[25], D. Utkin[24], A. Valkárová[32], C. Vallée[21], P. Van Mechelen[3], A. Vargas Trevino[6], Y. Vazdik[25], C. Veelken[17], S. Vinokurova[9], V. Volchinski[37], K. Wacker[6], G. Weber[10], R. Weber[39], D. Wegener[6], C. Werner[12], M. Wessels[9], B. Wessling[9], Ch. Wissing[6], R. Wolf[12], E. Wünsch[9], S. Xella[40], W. Yan[9], V. Yeganov[37], J. Žáček[32], J. Zálešák[31], Z. Zhang[27], A. Zhelezov[24], A. Zhokin[24], Y.C. Zhu[9], J. Zimmermann[26], T. Zimmermann[39], H. Zohrabyan[37], and F. Zomer[27]

[1] *I. Physikalisches Institut der RWTH, Aachen, Germany*[a]
[2] *School of Physics and Astronomy, University of Birmingham, Birmingham, UK*[b]
[3] *Inter-University Institute for High Energies ULB-VUB, Brussels; Universiteit Antwerpen, Antwerpen; Belgium*[c]
[4] *Rutherford Appleton Laboratory, Chilton, Didcot, UK*[b]
[5] *Institute for Nuclear Physics, Cracow, Poland*[d]
[6] *Institut für Physik, Universität Dortmund, Dortmund, Germany*[a]
[7] *Joint Institute for Nuclear Research, Dubna, Russia*
[8] *CEA, DSM/DAPNIA, CE-Saclay, Gif-sur-Yvette, France*
[9] *DESY, Hamburg, Germany*
[10] *Institut für Experimentalphysik, Universität Hamburg, Hamburg, Germany*[a]
[11] *Max-Planck-Institut für Kernphysik, Heidelberg, Germany*
[12] *Physikalisches Institut, Universität Heidelberg, Heidelberg, Germany*[a]
[13] *Kirchhoff-Institut für Physik, Universität Heidelberg, Heidelberg, Germany*[a]
[14] *Institut für Experimentelle und Angewandte Physik, Universität Kiel, Kiel, Germany*
[15] *Institute of Experimental Physics, Slovak Academy of Sciences, Košice, Slovak Republic*[f]
[16] *Department of Physics, University of Lancaster, Lancaster, UK*[b]
[17] *Department of Physics, University of Liverpool, Liverpool, UK*[b]
[18] *Queen Mary and Westfield College, London, UK*[b]
[19] *Physics Department, University of Lund, Lund, Sweden*[g]
[20] *Physics Department, University of Manchester, Manchester, UK*[b]
[21] *CPPM, CNRS/IN2P3 - Univ. Mediterranee, Marseille - France*
[22] *Departamento de Fisica Aplicada, CINVESTAV, Mérida, Yucatán, México*[j]
[23] *Departamento de Fisica, CINVESTAV, México*[j]
[24] *Institute for Theoretical and Experimental Physics, Moscow, Russia*[k]
[25] *Lebedev Physical Institute, Moscow, Russia*[e]
[26] *Max-Planck-Institut für Physik, München, Germany*
[27] *LAL, Université de Paris-Sud 11, IN2P3-CNRS, Orsay, France*
[28] *LLR, Ecole Polytechnique, IN2P3-CNRS, Palaiseau, France*
[29] *LPNHE, Universités Paris VI and VII, IN2P3-CNRS, Paris, France*
[30] *Faculty of Science, University of Montenegro, Podgorica, Serbia and Montenegro*[e]
[31] *Institute of Physics, Academy of Sciences of the Czech Republic, Praha, Czech Republic*[h]
[32] *Faculty of Mathematics and Physics, Charles University, Praha, Czech Republic*[h]
[33] *Dipartimento di Fisica Università di Roma Tre and INFN Roma 3, Roma, Italy*
[34] *Institute for Nuclear Research and Nuclear Energy, Sofia, Bulgaria*[e]
[35] *Paul Scherrer Institut, Villigen, Switzerland*
[36] *Fachbereich C, Universität Wuppertal, Wuppertal, Germany*
[37] *Yerevan Physics Institute, Yerevan, Armenia*
[38] *DESY, Zeuthen, Germany*
[39] *Institut für Teilchenphysik, ETH, Zürich, Switzerland*[i]
[40] *Physik-Institut der Universität Zürich, Zürich, Switzerland*[i]

[41] *Also at Physics Department, National Technical University, Zografou Campus, GR-15773 Athens, Greece*
[42] *Also at Rechenzentrum, Universität Wuppertal, Wuppertal, Germany*
[43] *Also at University of P.J. Šafárik, Košice, Slovak Republic*
[44] *Also at CERN, Geneva, Switzerland*
[45] *Also at Max-Planck-Institut für Physik, München, Germany*
[46] *Also at Comenius University, Bratislava, Slovak Republic*

[†] *Deceased*

[a] *Supported by the Bundesministerium für Bildung und Forschung, FRG, under contract numbers 05 H1 1GUA /1, 05 H1 1PAA /1, 05 H1 1PAB /9, 05 H1 1PEA /6, 05 H1 1VHA /7 and 05 H1 1VHB /5*
[b] *Supported by the UK Particle Physics and Astronomy Research Council, and formerly by the UK Science and Engineering Research Council*
[c] *Supported by FNRS-FWO-Vlaanderen, IISN-IIKW and IWT and by Interuniversity Attraction Poles Programme, Belgian Science Policy*
[d] *Partially Supported by the Polish State Committee for Scientific Research, SPUB/DESY/P003/DZ 118/2003/2005*
[e] *Supported by the Deutsche Forschungsgemeinschaft*
[f] *Supported by VEGA SR grant no. 2/4067/ 24*
[g] *Supported by the Swedish Natural Science Research Council*
[h] *Supported by the Ministry of Education of the Czech Republic under the projects LC527 and INGO-1P05LA259*
[i] *Supported by the Swiss National Science Foundation*
[j] *Supported by CONACYT, México, grant 400073-F*
[k] *Partially Supported by Russian Foundation for Basic Research, grants 03-02-17291 and 04-02-16445*

1 Introduction

Doubly-charged Higgs bosons ($H^{\pm\pm}$) appear when the Higgs sector of the Standard Model (SM) is extended by one or more triplet(s) with non-zero hypercharge [1–3]. Examples are provided by some Left-Right Symmetric models [4], or their supersymmetric extensions, which are of particular interest since they provide a mechanism to generate small non-zero neutrino masses. Such models can lead to a doubly-charged Higgs boson light enough [5] to be produced at the existing colliders. The Higgs triplet(s) may be coupled to matter fields via Yukawa couplings which are generally not related to the fermion masses. A non-vanishing coupling of a doubly-charged Higgs to an electron would allow its single production in ep collisions at HERA. This possibility is investigated in this paper with a search for doubly-charged Higgs bosons decaying into a high mass pair of same charge leptons, one of them being an electron.

An analysis of multi-electron events was already presented by the H1 collaboration [6]. Six events were observed with a di-electron mass above 100 GeV, a domain in which the Standard Model prediction is low. In the present paper the compatibility of these events with the hypothesis of a doubly-charged Higgs coupling to ee is addressed and a further search for a $H^{\pm\pm}$ boson coupling to $e\mu$ and $e\tau$ is performed. The analysis is based on ep data collected by the H1 experiment between 1994 and 2000, which amount to a luminosity of up to 118 pb^{-1}.

2 Phenomenology

At tree level, doubly-charged Higgs bosons couple only to charged leptons and to other Higgs and gauge bosons. Couplings to quark pairs are forbidden by charge conservation. The couplings of a doubly-charged Higgs to charged leptons can be generically described by the Lagrangian:

$$\mathcal{L} = \sum_{i,j} h^{L,R}_{l_i l_j} \, H^{++}_{L,R} \, \bar{l}^{\,c}_i \, P_{L,R} \, l_j \qquad + \text{ h.c. } , \tag{1}$$

where l are the charged lepton fields, l^c denote the charge conjugate fields, i, j are generation indices, and $P_{L,R} = (1 \mp \gamma_5)/2$. The Higgs fields $H^{++}_{L,R}$ coupling to left-handed or right-handed leptons correspond to different particles and not all models predict their simultaneous existence. The Yukawa couplings $h^{L,R}_{l_i l_j} = h^{L,R}_{l_j l_i}$ are free parameters of the model.

The phenomenology of doubly-charged Higgs production at HERA was first discussed in [7]. For a non-vanishing coupling $h^{L,R}_{el}$ the single production of a doubly-charged Higgs boson is possible at HERA in $e\gamma^*$ interactions via the diagrams shown in Fig. 1, where a photon is radiated off the proton or one of its constituent quarks. The proton may remain intact or be broken during this interaction, leading to an elastic or inelastic reaction, respectively. With longitudinally unpolarised lepton beams, as were delivered by HERA until 2000, the $H^{\pm\pm}$ production cross section does not depend on whether the Higgs couples to left-handed or right-handed leptons. Hence a generic case is considered here of a doubly-charged Higgs boson which couples to either left-handed or right-handed leptons and the L, R indices are dropped in the following.

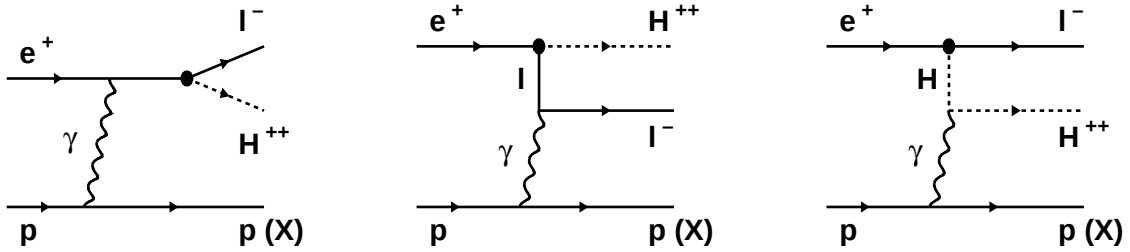

Figure 1: Diagrams for the single production of a doubly-charged Higgs boson in e^+p collisions at HERA via the h_{el} coupling. The hadronic final state is denoted by p (X) in the elastic (inelastic) case, where the initial proton remains intact (dissociates). The contribution of Z exchange can be safely neglected.

Within the mass range considered in this analysis, it is assumed that decays of the $H^{\pm\pm}$ into gauge bosons and other Higgs particles are not allowed kinematically such that the doubly-charged Higgs only decays via its Yukawa couplings into a lepton pair.

Indirect upper bounds on the Yukawa couplings of a doubly-charged Higgs to leptons are reviewed in [8]. The coupling h_{ee} of a doubly-charged Higgs to an electron pair is constrained by the contribution of virtual $H^{\pm\pm}$ exchange to Bhabha scattering in e^+e^- collisions. A recent OPAL analysis [9] sets the constraint $h_{ee} < 0.14$ for a doubly-charged Higgs mass $M_H = 100$ GeV. From low energy e^+e^- data, coupling values of $\mathcal{O}(0.1)$ are allowed for $h_{e\mu}$ and $h_{e\tau}$ for a Higgs mass of 100 GeV [10]. Taking these indirect constraints into account, the production of a doubly-charged Higgs mediated by h_{ee}, $h_{e\mu}$ or $h_{e\tau}$ might be observable at HERA. The Higgs signal would manifest itself as a peak in the invariant mass distribution of same charge ee, $e\mu$ or $e\tau$ leptons, respectively. For the range of masses and couplings probed in this analysis, the Higgs decay length is vanishingly small but its width remains negligible compared to the experimental resolution on the mass of the lepton pair.

3 Simulation of the Signal and Standard Model Backgrounds

The calculation of the cross section for doubly-charged Higgs production, as well as the simulation of signal events, relies on a dedicated Monte Carlo program developed for this analysis. The differential cross sections are integrated using the VEGAS package [11]. Different approaches are followed depending on the photon virtuality Q^2 and on the mass W of the hadronic final state:

- in the inelastic region ($W > m_p + m_\pi$, with the proton mass m_p and the pion mass m_π) and when the photon virtuality is large ($Q^2 > 4$ GeV^2), the interaction involves a quark inside the proton. The squared amplitude of the process $e^\pm q \to e^\mp H^{\pm\pm} q$ is evaluated using the CompHEP package [12, 13]. The parton densities in the proton are taken from the CTEQ4L [14] parameterisation and are evaluated at the scale $\sqrt{Q^2}$. The parton shower approach [15] based on the DGLAP [16] evolution equations is applied to

simulate QCD corrections in the initial and final states, and the hadronisation is performed using PYTHIA 6.1 [15].

- for the elastic region (W = m_p) and the inelastic region at low Q^2 ($W > m_p + m_\pi$, $Q^2 < 4$ GeV^2), the squared amplitude is calculated using the FORM program [17]. The hadronic tensor is parameterised in terms of the usual electromagnetic structure functions $F_1(x, Q^2)$ and $F_2(x, Q^2)$ of the proton, where $x = Q^2/(W^2 + Q^2 - m_p^2)$. For the elastic process these structure functions are expressed in terms of the electric and magnetic form factors of the proton. For the low Q^2 inelastic region they are taken from analytical parameterisations [18]. The simulation of the hadronic final state for low Q^2 inelastic events is performed via an interface to the SOPHIA program [19].

For a Yukawa coupling h_{ee} or $h_{e\mu}$ of electromagnetic strength ($h = \sqrt{4\pi\alpha_{em}} = 0.3$) the total cross section amounts to 0.39 pb (0.04 pb) for a Higgs mass of 100 GeV (150 GeV). The low Q^2 (high Q^2) inelastic contribution is found to be $\sim 30\%$ ($\sim 20\%$) of the total cross section in the mass range $80 - 150$ GeV. The cross section for producing a doubly-charged Higgs via a coupling $h_{e\tau}$ is lower by about 40% due to the non-negligible mass of the τ lepton produced in association with the Higgs.

The theoretical uncertainty on the cross sections obtained is taken to be 4% in the mass range considered. This is derived from an assessed uncertainty of 2% on the proton form factors [20] and from the uncertainty on the scale at which the parton densities for the inelastic contribution are evaluated. The latter uncertainty is estimated from the variation of the computed cross section as this scale is changed from $\sqrt{Q^2}/2$ to $2\sqrt{Q^2}$.

Separate signal event samples corresponding to the production and decay of a doubly-charged Higgs via a coupling h_{ee}, $h_{e\mu}$ and $h_{e\tau}$ have been produced for Higgs masses ranging between 80 and 150 GeV, in steps of 10 GeV.

Di-electron production, which proceeds mainly via two-photon interactions, constitutes an irreducible background for ee final states. The production of muon or tau pairs constitutes a background for the $e\mu$ and $e\tau$ analyses when the scattered electron is detected. The Cabibbo-Parisi process $ee \to \gamma, Z \to ll$, in which the incoming electron interacts with an electron emitted from a photon radiated from the proton, contributes at high transverse momentum only. The Drell-Yan process was calculated in [21] and found to be negligible. All these processes are simulated using the GRAPE Monte Carlo generator [22], which also takes into account contributions from Bremsstrahlung with subsequent photon conversion into a lepton pair and electroweak contributions.

Experimental backgrounds come dominantly from Neutral Current Deep Inelastic Scattering (NC DIS) where a jet is misidentified as an electron, a muon or a tau. Compton scattering is also a source of background for ee final states when the photon is misidentified as an electron. These processes are simulated with the DJANGO [23] and WABGEN [24] generators.

All generated events are passed through the full simulation of the H1 apparatus and are reconstructed using the same program chain as for the data.

4 The H1 Detector

A detailed description of the H1 experiment can be found in [25]. Only the H1 detector components relevant to the present analysis are briefly described here. Jets and electrons are measured with the Liquid Argon (LAr) calorimeter [26], which covers the polar angle[1] range $4^\circ < \theta < 154^\circ$. Electromagnetic shower energies are measured with a precision of $\sigma(E)/E = 12\%/\sqrt{E/\text{GeV}} \oplus 1\%$ and hadronic energies with $\sigma(E)/E = 50\%/\sqrt{E/\text{GeV}} \oplus 2\%$, as determined in test beams [27]. In the backward region a lead/scintillating-fibre[2] (SpaCal) calorimeter [28] covers the range $155^\circ < \theta < 178^\circ$. The central ($20^\circ < \theta < 160^\circ$) and forward ($7^\circ < \theta < 25^\circ$) tracking detectors are used to measure charged particle trajectories, to reconstruct the interaction vertex and to supplement the measurement of the hadronic energy. The LAr and inner tracking detectors are enclosed in a super-conducting magnetic coil with a strength of 1.15 T. The return yoke of the coil is the outermost part of the detector and is equipped with streamer tubes forming the central muon detector ($4^\circ < \theta < 171^\circ$). In the forward region of the detector ($3^\circ < \theta < 17^\circ$) a set of drift chamber layers (the forward muon system) detects muons and, together with an iron toroidal magnet, allows a momentum measurement. The luminosity measurement is based on the Bethe-Heitler process $ep \to ep\gamma$, where the photon is detected in a calorimeter located downstream of the interaction point.

5 Data Analysis

The analyses of ee and $e\mu$ final states use the full $e^{\pm}p$ data set recorded in the period 1994-2000, which corresponds to an integrated luminosity of $118\,\text{pb}^{-1}$. The analysis of $e\tau$ final states makes use of the $e^{+}p$ data collected in the years 1996-1997 and 1999-2000, which amount to a luminosity of $88\,\text{pb}^{-1}$. The HERA collider was operated at a centre-of-mass energy $\sqrt{s}$ of 300 GeV in 1994-1997 and of 318 GeV in 1998-2000.

Events are first selected by requiring that the longitudinal position of the vertex be within 35 cm around the nominal interaction point. In addition topological filters and timing vetoes are applied to remove background events induced by cosmic showers and other non-ep sources. The main triggers for the events are provided by the LAr calorimeter and the muon system.

5.1 Lepton Identification

An electron[3] candidate is identified by the presence of a compact and isolated electromagnetic energy deposit above 5 GeV in the LAr or SpaCal calorimeter. The energy of the electron candidate is measured from the calorimetric information. In the angular range $20^\circ < \theta < 150^\circ$ the electron identification is complemented by tracking conditions, in which case the direction

[1] The origin of the H1 coordinate system is the nominal ep interaction point, with the direction of the proton beam defining the positive z-axis (forward region). The transverse momenta are measured in the xy plane. The pseudorapidity η is related to the polar angle θ by $\eta = -\ln \tan(\theta/2)$.

[2] Before 1995 a lead-scintillator calorimeter was used.

[3] Unless otherwise stated, the term "electron" is used in this paper to generically describe electrons or positrons.

of the electron candidate is given by that of the associated track. Electron candidates in the forward region, $5^\circ < \theta < 20^\circ$, are required to have an energy above 10 GeV.

A muon candidate is identified by associating an isolated track in the forward muon system or in the inner tracking system with a track segment or an energy deposit in the instrumented iron. The muon momentum is measured from the track curvature in the toroidal or solenoidal magnetic field, respectively.

Tau leptons are preselected as described in [29] by requiring a track with transverse momentum above 5 GeV measured in the inner tracking detector. The leptonic tau decays $\tau \to e\nu\nu$ and $\tau \to \mu\nu\nu$ are reconstructed by matching the selected track to an identified electron or muon. Tracks that are not identified as electrons or muons are attributed to hadronic tau decays if at least 40% of the track momentum is reconstructed in the LAr calorimeter as matched clustered energy. In that case it is moreover required that the track belong to a narrow jet: no other track should be reconstructed within $0.15 < R < 1.5$ around the track direction, where $R = \sqrt{\Delta\eta^2 + \Delta\varphi^2}$ with $\Delta\eta$ and $\Delta\varphi$ being the distances in pseudorapidity and azimuthal angle, respectively. The transverse momentum and the direction of the τ candidate are approximated by those of the associated track.

5.2 Analysis of the $H \to ee$ Decay

This analysis is based on the published H1 measurement of multi-electron production [6]. The event selection requires at least two central ($20^\circ < \theta^e < 150^\circ$) electron candidates, one of them with a transverse momentum $P_T^{e1} > 10$ GeV (ensuring a trigger efficiency close to 100% [30]) and the other one with $P_T^{e2} > 5$ GeV. After this preselection, 125 events are observed, in good agreement with the SM expectation of 137.4 ± 10.7. In each event, the two highest P_T electrons, one of those being possibly outside the central region, are assigned to the Higgs candidate. The distribution of their invariant mass M_{ee} is shown in Fig. 2a. At low mass a good agreement is observed between data and the SM expectation which is largely dominated by $\gamma\gamma$ contributions. Six events are observed at $M_{ee} > 100$ GeV, compared to the SM expectation of 0.53 ± 0.08.

Further selection criteria are then applied, which are designed to maximise the sensitivity of the analysis to a possible $H^{\pm\pm}$ signal. The charge measurement of the two leptons assigned to the Higgs candidate is exploited. In e^+p (e^-p) collisions, where H^{++} (H^{--}) bosons could be produced, events in which one of the two leptons is reliably assigned a negative (positive) charge are rejected. The charge assignment requires that the curvature κ of the track associated with the lepton be measured with an error $\delta\kappa$ satisfying $\mid \kappa/\delta\kappa \mid > 2$. The precise calorimetric measurement of the electron transverse momenta is further exploited by applying an additional M_{ee} dependent cut on the sum of the transverse momenta of the two electrons assigned to the Higgs candidate. The lower bound is optimised to keep 95% of the signal and varies between 45 GeV and 120 GeV. This cut suppresses events coming from $\gamma\gamma$ processes. The efficiency for selecting signal events varies from 50% for a $H^{\pm\pm}$ mass of 80 GeV to 35% for a $H^{\pm\pm}$ mass of 150 GeV. In this mass range the resolution on M_{ee} varies between 2.5 GeV and 5 GeV.

After these requirements, 3 events are observed at $M_{ee} > 65$ GeV, in agreement with the SM expectation of 2.45 ± 0.11 events. Amongst the six events[4] at $M_{ee} > 100$ GeV, only one satisfies the final selection criteria.

[4]Out of these, three do not fullfill the M_{ee} dependent P_T cut, and two do not satisfy the charge requirement.

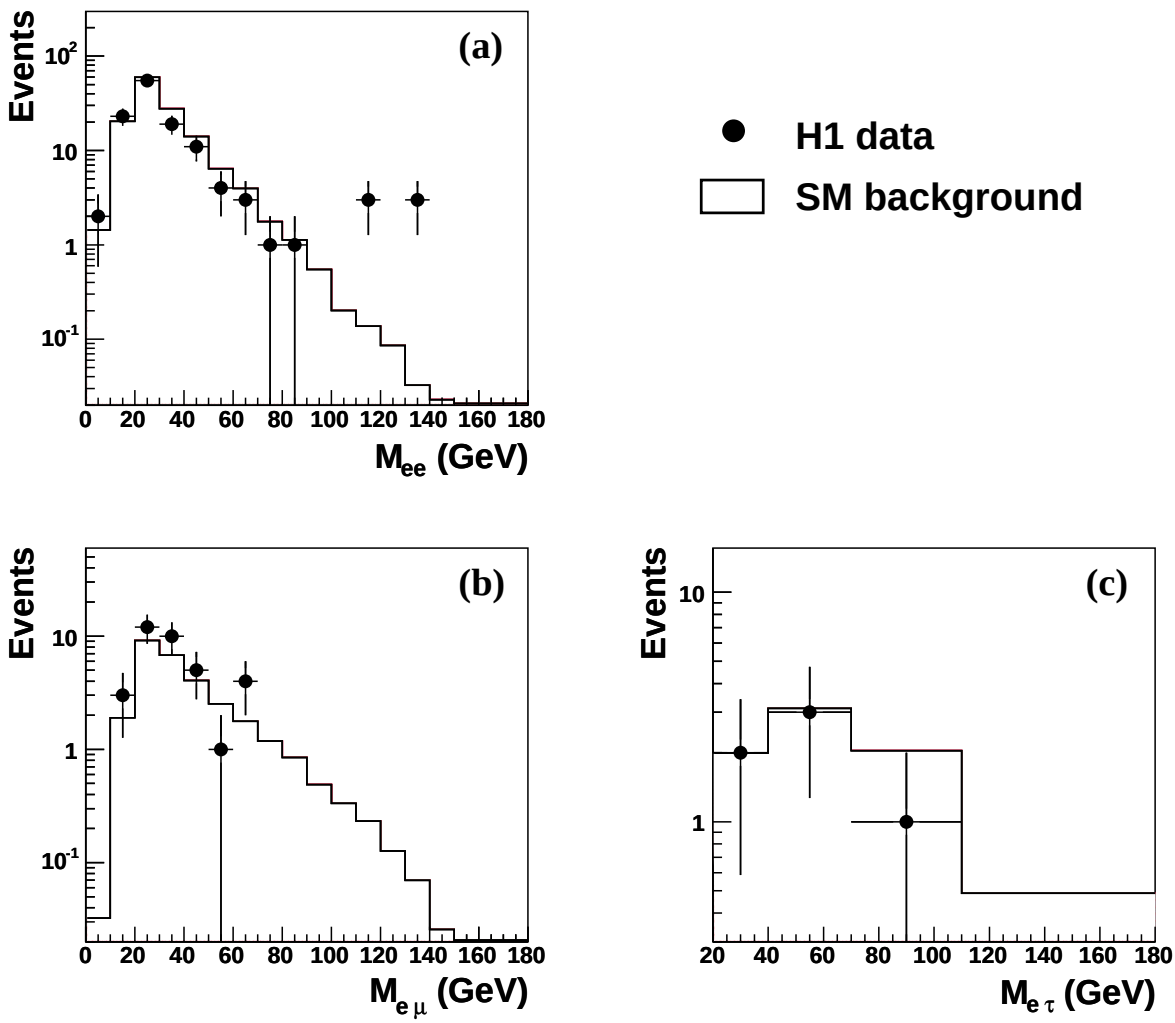

Figure 2: Distribution of (a) the invariant mass M_{ee} of the two highest P_T electrons for multi-electron events, (b) the electron-muon invariant mass $M_{e\mu}$, and (c) the electron-tau candidate invariant mass $M_{e\tau}$. The data (symbols) are compared with the Standard Model expectation (histogram). The distributions are shown at the preselection level (see text).

5.3 Analysis of the $H \to e\mu$ Decay

Events having one electron and one muon with minimal transverse momenta of $P_T^e > 10$ GeV and $P_T^\mu > 5$ GeV are selected. The polar angle of electron candidates is restricted to $20^\circ < \theta^e < 140^\circ$ to reduce the large background arising from NC DIS events. The θ range for muon candidates extends towards low angles, $10^\circ < \theta^\mu < 140^\circ$, which increases the efficiency for high $H^{\pm\pm}$ masses. The minimum transverse momentum required for electron candidates ensures a trigger efficiency close to 100% for these events. After this preselection, 35 data events are observed compared to a SM expectation of 29.6 ± 3.4. The distribution of the invariant mass of the electron and the muon $M_{e\mu}$ is shown in Fig. 2b. A good agreement is observed between the data and the SM expectation, which is dominated by $\gamma\gamma$ contributions.

For the final selection of $H \to e\mu$ candidates the charge of the e and μ is exploited using the same criteria as used in section 5.2. The efficiency for selecting signal events varies from 55%

to 40% for a $H^{\pm\pm}$ mass between 80 GeV and 150 GeV. The resolution on $M_{e\mu}$ varies between 3 GeV and 8 GeV. For $M_{e\mu} > 65$ GeV one event is observed while 4.17 ± 0.44 events are expected from the SM.

5.4 Analysis of the $H \rightarrow e\tau$ Decay

The search for a H^{++} boson decaying into $e\tau$ is performed in three final states, depending on whether the τ decays into an electron, a muon or hadronically (h). Details of this analysis can be found in [29]. Events are selected which contain either two electrons (ee), or an electron and a muon ($e\mu$), or an electron and a hadronic τ candidate (eh) as defined in section 5.1. The two leptons, or the electron and the hadronic-τ candidate, should have a transverse momentum above 5 GeV, be in the angular range $20^\circ < \theta < 140^\circ$, and be separated from each other by $R > 2.5$ in pseudorapidity-azimuth. One of them must have a transverse momentum above 10 GeV, which ensures a trigger efficiency above 95% in all three classes. For events in the $e\mu$ class the polar angle of the electron candidate is required to be below 120°.

A significant amount of missing transverse and longitudinal momentum is expected due to the neutrinos produced in the τ decays. Events in the ee class are required to have a missing transverse momentum $P_T^{miss} > 8$ GeV. For the eh class, which suffers from a large NC DIS background, it is required that $P_T^{miss} > 11$ GeV, that the energy deposited in the SpaCal calorimeter be below 5 GeV, and that the variable $\sum_i E^i - P_z^i$, where the sum runs over all visible particles, be smaller than 49 GeV. For fully contained events $\sum_i E^i - P_z^i$ is expected to peak at twice the lepton beam energy $E_0 = 27.5$ GeV, i.e. 55 GeV, while signal events are concentrated at lower values due to the non observed neutrinos. In total 6 events are preselected, in agreement with the SM prediction of 7.8 ± 1.5.

In each class, the $e\tau$ invariant mass $M_{e\tau}$ is reconstructed by imposing longitudinal momentum and energy conservation, and by minimising the total momentum imbalance in the transverse plane. Tau leptons are assumed to decay with a vanishing opening angle. This method yields a resolution of about 4 GeV on the mass $M_{e\tau}$. Figure 2c shows the $e\tau$ invariant mass distribution of the selected events together with the SM expectation.

For the final selection, events are rejected if the track associated with one of the Higgs decay product candidates is reliably assigned a negative charge, opposite to that of the incoming lepton beam. The signal efficiencies depend only weakly on M_H. The fractions of simulated $H \rightarrow e\tau$ events which are reconstructed in the various classes are given in table 1, for an example mass of $M_H = 100$ GeV. The total efficiency on the signal amounts to about 25%.

The final event yields are also shown in table 1. Only one event (in the eh class) satisfies the final criteria, while 2.1 ± 0.5 events are expected.

5.5 Systematic Uncertainties

The systematic uncertainties attributed to the Monte Carlo predictions for the ee analysis are detailed in [6]. The dominant systematic uncertainty is due to the electron-track association efficiency, which is 90% on average with an uncertainty increasing with decreasing polar angle

Event class	$H^{++} \to e^+\tau^+$ final selection		
	N_{obs}	N_{bckg}	Signal fraction
$e\mu$	0	0.27$\pm$ 0.02	6 %
eh	1	1.66 $\pm$ 0.48	12 %
ee	0	0.14$\pm$ 0.04	7 %
total	1	2.07$\pm$ 0.54	25 %

Table 1: Number of observed (N_{obs}) and expected (N_{bckg}) events in each event class which satisfy all criteria to select $H^{++} \to e^+\tau^+$ candidates with a mass $M_{e\tau} > 65$ GeV. The last column shows the fractions of the $H \to e\tau$ Monte Carlo events which are reconstructed in the various classes, for a mass of 100 GeV.

from 3% to 15%. Systematic errors due to the uncertainty on the electromagnetic energy scale (known at the 0.7% to 3% level in the central and forward regions of the LAr calorimeter, respectively) and on the trigger efficiency (3%) are also taken into account.

For the $e\mu$ analysis, the dominant additional systematic uncertainty is due to the muon identification efficiency known within 6% [31]. The uncertainty due to the reconstruction efficiency of the central tracking detector for central muons contributes an additional 3%. The muon momentum scale is known within 5%, and the trigger efficiency for $e\mu$ final states is known within 3%.

The same systematic uncertainties affect the SM expectations in the ee and $e\mu$ classes of the $e\tau$ analysis. The uncertainty of the hadronic energy scale in the LAr calorimeter (4%) constitutes another source of uncertainty due to the cuts applied on the P_T^{miss} and $\sum_i E - P_z$ variables. For the eh event class the dominant uncertainties on the SM expectation, coming mainly from NC DIS processes, are due to the uncertainty of 3% of the track efficiency, to that of the hadronic energy scale, and to that of the hadronisation model.

The luminosity measurement leads to a normalisation uncertainty of 1.5%.

For both the expected signal and the predicted background, the systematic uncertainties resulting from the sources listed above are added in quadrature.

6 Interpretation

With the final Higgs selection no significant excess over the SM expectation is observed. Upper limits on the $H^{\pm\pm}$ production cross section times the branching ratio for the $H^{\pm\pm}$ to decay into one of the analysed final states are derived as a function of the $H^{\pm\pm}$ mass and are shown in Fig. 3a. The limits are presented at the 95% confidence level and are obtained using a modified frequentist approach [32]. Statistical uncertainties, as well as the influence of the various systematic uncertainties on both the shape and the normalisation of the mass distributions for signal and background events, are taken into account. The best sensitivity is obtained for a $H^{\pm\pm}$ produced and decaying via $h_{e\mu}$, with upper limits around 0.05 pb.

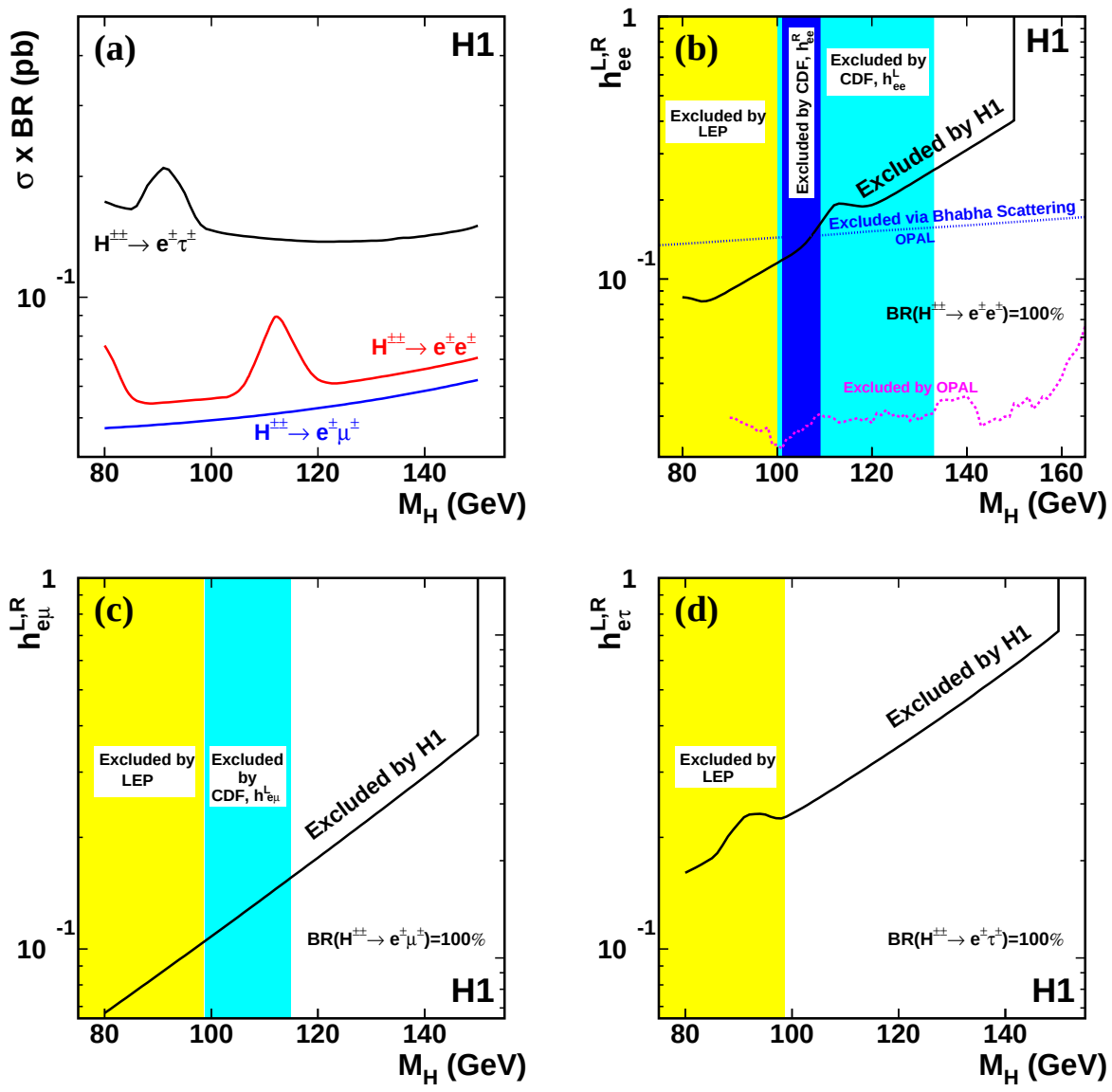

Figure 3: (a) Upper limits at the 95% confidence level on the $H^{\pm\pm}$ production cross section times the branching ratio for the $H^{\pm\pm}$ to decay into ee, $e\mu$ or $e\tau$, as a function of the Higgs mass. (b)-(d) Upper limits on the coupling h_{el} assuming that the $H^{\pm\pm}$ couples only (b) to ee, (c) to $e\mu$ or (d) to $e\tau$. Regions above the curves are excluded. The constraints obtained from pair production at LEP and at CDF and from single production at OPAL are also shown.

Assuming that only one Yukawa coupling h_{el} is non-vanishingly small, these constraints are translated into mass dependent upper limits on the coupling h_{el}, as shown in Fig. 3b-d.

If the doubly-charged Higgs boson couples only to an electron pair (Fig. 3b) the ee analysis rules out $H^{\pm\pm}$ masses below 138 GeV for a coupling h_{ee} of the electromagnetic strength, $h_{ee} = 0.3$. The result is compared to the bounds obtained from searches for $H^{\pm\pm}$ pair production at LEP [33] and by the CDF experiment [34], and to both the indirect and direct limits obtained by the OPAL experiment [9], the latter being the most stringent. The OPAL experiment has also set

similar stringent constraints on h_{ee} independently of the Higgs decay mode. These constraints also exclude a sizeable $H^{\pm\pm}$ production at HERA via h_{ee} followed by the $H^{\pm\pm}$ decay via $h_{\mu\mu}$ or $h_{\tau\tau}$, which is consistent with the non-observation of a resonance signal in the $\mu\mu$ [31] and $\tau\tau$ [29] final states in the present H1 data.

Assuming that the doubly-charged Higgs boson couples only to an electron-muon (electron-tau) pair, the $e\mu$ ($e\tau$) analysis allows masses below 141 GeV (112 GeV) to be ruled out for $h_{e\mu} = 0.3$ ($h_{e\tau} = 0.3$), as shown in Fig. 3c (Fig. 3d). The H1 limits extend the excluded region in the electron-muon and electron-tau channels to masses that are beyond those reached in previous searches for pair production at LEP [33] and the Tevatron [34].

7 Conclusion

A search for the single production of doubly-charged Higgs bosons coupling to ee, $e\mu$ or $e\tau$ is presented. In a previous model independent multi-electron analysis, H1 observed six events with a di-electron mass above 100 GeV, a region where the Standard Model expectation is small. Out of the six events, only one is compatible with the signature of a doubly-charged Higgs boson. No electron-muon or electron-tau event is found in this mass domain.

This analysis places new limits on the $H^{\pm\pm}$ mass and its Yukawa couplings h_{el} to an electron-lepton pair. Assuming that the doubly-charged Higgs boson only couples to electron-muon (electron-tau) pairs, a limit of 141 GeV (112 GeV) is obtained on the Higgs mass, for a coupling $h_{e\mu} = 0.3$ ($h_{e\tau} = 0.3$) corresponding to an interaction of electromagnetic strength.

Acknowledgements

We are grateful to the HERA machine group whose outstanding efforts have made this experiment possible. We thank the engineers and technicians for their work in constructing and maintaining the H1 detector, our funding agencies for financial support, the DESY technical staff for continual assistance and the DESY directorate for support and for the hospitality which they extend to the non-DESY members of the collaboration. We are especially grateful to J. Maalampi and N. Romanenko for providing the doubly-charged Higgs Lagrangian implementation in CompHEP which was used in this analysis. We would also like to thank K. Huitu and E. Boos for their help and valuable discussions.

References

[1] G. B. Gelmini and M. Roncadelli, Phys. Lett. B **99** (1981) 411.

[2] J. C. Pati and A. Salam, Phys. Rev. D **10** (1974) 275; R. E. Marshak and R. N. Mohapatra, Phys. Lett. B **91** (1980) 222.

[3] R. N. Mohapatra and G. Senjanovic, Phys. Rev. Lett. **44** (1980) 912.

[4] G. Senjanovic and R. N. Mohapatra, Phys. Rev. D **12** (1975) 1502; R. N. Mohapatra and R. E. Marshak, Phys. Rev. Lett. **44** (1980) 1316 [Erratum-ibid. **44** (1980) 1643].

[5] C. S. Aulakh, A. Melfo and G. Senjanovic, Phys. Rev. D **57** (1998) 4174 [hep-ph/9707256]; Z. Chacko and R. N. Mohapatra, Phys. Rev. D **58** (1998) 015003 [hep-ph/9712359]; B. Dutta and R. N. Mohapatra, Phys. Rev. D **59** (1999) 015018 [hep-ph/9804277].

[6] A. Aktas *et al.* [H1 Collaboration], Eur. Phys. J. C **31** (2003) 17 [hep-ex/0307015].

[7] E. Accomando and S. Petrarca, Phys. Lett. B **323** (1994) 212 [hep-ph/9401242].

[8] M. L. Swartz, Phys. Rev. D **40** (1989) 1521; J. F. Gunion *et al.*, Phys. Rev. D **40** (1989) 1546; M. Lusignoli and S. Petrarca, Phys. Lett. B **226** (1989) 397; G. Barenboim, K. Huitu, J. Maalampi and M. Raidal, Phys. Lett. B **394** (1997) 132 [hep-ph/9611362]; S. Godfrey, P. Kalyniak and N. Romanenko, Phys. Rev. D **65** (2002) 033009 [hep-ph/0108258].

[9] G. Abbiendi *et al.* [OPAL Collaboration], Phys. Lett. B **577** (2003) 93 [hep-ex/0308052].

[10] F. Cuypers and S. Davidson, Eur. Phys. J. C **2** (1998) 503.

[11] G.P. Lepage, CLNS-80/447 (1980).

[12] E. Boos *et al.* [CompHEP Collaboration], Nucl. Instrum. Meth. A **534** (2004) 250 [hep-ph/0403113]; A. Pukhov *et al.*, "CompHEP - a package for evaluation of Feynman diagrams and integration over multi-particle phase space", hep-ph/9908288; available at http://theory.sinp.msu.ru/comphep.

[13] S. Godfrey, P. Kalyniak and N. Romanenko, Phys. Rev. D **65** (2002) 033009 [hep-ph/0108258].

[14] H. L. Lai *et al.*, Phys. Rev. D **55** (1997) 1280 [hep-ph/9606399].

[15] T. Sjöstrand *et al.*, Comput. Phys. Commun. **135** (2001) 238 [hep-ph/0010017].

[16] V. N. Gribov and L. N. Lipatov, Yad. Fiz. **15** (1972) 781 [Sov. J. Nucl. Phys. **15** (1972) 438]; G. Altarelli and G. Parisi, Nucl. Phys. B **126** (1977) 298; Y. L. Dokshitzer, Sov. Phys. JETP **46** (1977) 641 [Zh. Eksp. Teor. Fiz. **73** (1977) 1216].

[17] J. A. M Vermaseren, "New features of FORM", math-ph/0010025.

[18] F.W. Brasse *et al.*, Nucl. Phys. B **39** (1972) 421.

[19] A. Mucke, R. Engel, J. P. Rachen, R. J. Protheroe and T. Stanev, Comput. Phys. Commun. **124** (2000) 290 [astro-ph/9903478].

[20] R. C. Walker *et al.*, Phys. Rev. D **49** (1994) 5671.

[21] N. Arteaga-Romero, C. Carimalo and P. Kessler, Z. Phys. C **52** (1991) 289.

[22] T. Abe, Comput. Phys. Commun. **136** (2001) 126 [hep-ph/0012029].

[23] DJANGO 6.2; G.A. Schuler and H. Spiesberger, Proc. of the Workshop Physics at HERA, W. Buchmüller and G. Ingelman (Editors), Vol. 3 p. 1419 (October 1991).

[24] Ch. Berger and P. Kandel, "A new Generator for Wide Angle Bremsstrahlung", Proc. of the Monte Carlo Generators for HERA Physics Workshop, A.T. Doyle, G. Grindhammer, G. Ingelman and H. Jung (Editors), DESY-PROC-1999-02, p. 596.

[25] I. Abt *et al.* [H1 Collaboration], Nucl. Instrum. Meth. A **386** (1997) 310 and 348.

[26] B. Andrieu *et al.* [H1 Calorimeter Group], Nucl. Instrum. Meth. A **336** (1993) 460.

[27] B. Andrieu *et al.* [H1 Calorimeter Group], Nucl. Instrum. Meth. A **344** (1994) 492; *idem*, Nucl. Instrum. Meth. A **350** (1994) 57; *idem*, Nucl. Instrum. Meth. A **336** (1993) 499.

[28] R. D. Appuhn *et al.* [H1 SPACAL Group], Nucl. Instrum. Meth. A **386** (1997) 397.

[29] S. Baumgartner, "Search for doubly-charged Higgs decaying into τ leptons at HERA", PhD thesis, ETH Zürich, ETH-16125 (2005), available at http://www-h1.desy.de/publications/theses_list.html.

[30] C. Adloff *et al.* [H1 Collaboration], Eur. Phys. J. C **30** (2003) 1 [hep-ex/0304003].

[31] A. Aktas *et al.* [H1 Collaboration], Phys. Lett. B **583** (2004) 28 [hep-ex/0311015].

[32] T. Junk, Nucl. Instr. Meth. A **434** (1999) 435 [hep-ex/9902006].

[33] J. Abdallah *et al.* [DELPHI Collaboration], Phys. Lett. B **552** (2003) 127 [hep-ex/0303026]; P. Achard *et al.* [L3 Collaboration], Phys. Lett. B **576** (2003) 18 [hep-ex/0309076]; G. Abbiendi *et al.* [OPAL Collaboration], Phys. Lett. B **526** (2002) 221 [hep-ex/0111059].

[34] D. Acosta *et al.* [CDF Collaboration], Phys. Rev. Lett. **93** (2004) 221802 [hep-ex/0406073].